Original Article

Optimization on submarine stern design

**Mohammad Moonesun[1,2], Yuri Mikhailovich Korol[1],
Hosein Dalayeli[3], Davood Tahvildarzade[3], Mehran Javadi[3],
Mohammad Jelokhaniyan[4] and Asghar Mahdian[3]**

Abstract

This article discusses the optimum hydrodynamic shape of the submarine stern based on the minimum resistance. Submarines consist of two major categories of hydrodynamic shape: the teardrop shape and the cylindrical middle-body shape. Due to the parallel middle-body shape in most of the naval submarines, those with cylindrical middle-body are studied here. The bare hull has three main parts: bow, cylinder and stern. This article proposes an optimum stern shape by the computational fluid dynamics method via Flow Vision software. In the hydrodynamic design point of view, the major parameters of the stern included the wake field (variation in fluid velocity) and resistance. The focus of this article is on the resistance at fully submerged mode without any regard for free surface effects. First, all the available equations for the stern shape of submarine are presented. Second, a computational fluid dynamics analysis has been performed according to the shape equations. For all the status, the following parameters are assumed to be constant: velocity, dimensions of domain, diameter, bow shape and total length (bow, middle and stern length).

Introduction

There are some rules and concepts about submarines and submersibles' shape design. There is an urgent need for understanding the basis and concepts of shape design. Submarine shape design is strictly dependent on the hydrodynamic characteristics such as other marine vehicles and ships. In submerged navigation, submarines are encountered with limited energy. Based on this fact, the minimum resistance is then vital in submarine hydrodynamic design. In addition, the shape design depends on the internal architecture and general arrangements of submarine. In real naval submarines, the submerged mode is the base for the determination of the hull form. Several parts of submarine are bare hull and sailing. The parts of bare hull are the bow, middle part and stern. The focus of this article is on this type of bare hull. Joubert[1,2] describes the notes of naval submarine shape design regarding the hydrodynamic aspects. The basis of submarine shape selection with all aspects such as general arrangement, hydrodynamic, dynamic stability, flow noise and sonar efficiency is discussed by Burcher and Rydill.[3] A lot of scientific material about naval submarine hull form and appendage

design with hydrodynamic considerations is presented by Yuri and Oleg[4] Some studies based on computational fluid dynamics (CFD) method about submarine hull form design with minimum resistance are done by Moonesun and colleagues[5–10] Special discussions about naval submarine shape design are presented in Iranian Hydrodynamic Series of Submarines (IHSS) (Moonesun,[6] Iranian Defense Standard (IDS-857:2011[11])). Some case study discussions based on CFD method about the hydrodynamic effects of the bow shape and the overall length of the submarine are presented by Praveen and Krishnankutty[12] and Suman et al.[13] Defence R&D Canada[14,15] has suggested a hull form equation for the bare hull, sailing and appendages

[1]Faculty of Ship Design, National University of Shipbuilding Admiral Makarov (NUOS), Nikolaev Ukraine
[2]Faculty of MUT, Marine Engineering College, Shahin Shahr, Iran
[3]Faculty of MUT, Mechanical Engineering College, Shahin Shahr, Iran
[4]Tarbiat Modarres University, Tehran, Iran

Corresponding author:
Mohammad Moonesun, Faculty of Ship Design, National University of Shipbuilding Admiral Makarov (NUOS), No.9, PGS, Nikolaev, Ukraine.
Email: m.moonesun@gmail.com

in the name of "DREA standard model." Alemayehu et al.,[16] Minnick[17] and Grant[18] present an equation for teardrop hull form with some of their limitations on coefficients, but the main source of their equation is presented by Jackson and Capt.[19] The simulation of the hull form with different coefficients is performed by Stenars.[20] Another equation for torpedo hull shape is presented by Prestero.[21] Formula "Myring" as a famous formula for axisymmetric shapes is presented by Myring.[22] Extensive experimental results about hydrodynamic optimization of teardrop or similar shapes are presented by Hoerner.[23] This reference is known as the main reference book in the field of the selection of aerodynamic and hydrodynamic shapes based on the experimental tests. Collective experimental studies about the shape design of bow and stern of the underwater vehicles that are based on the underwater missiles are presented by Greiner.[24] Most parts of this book are useful in the field of naval submarine shape design. Other experimental studies on the several teardrop shapes of submarines are presented by Denpol.[25] All equations of hull form, sailing and appendages for SUBOFF project with the experimental and CFD results are presented by Groves et al.[26] and Roddy.[27] Jerome et al.[28] and Brenden[29] have studied the optimization of submarine shape according to a logical algorithm based on minimum resistance. Optimization of shape based on minimum resistance in snorkel depth is studied by Volker and Alvarez.[30] Evaluation of optimum body form and bow shape for minimizing the resistance in submerged mode is performed by Moonesun et al.[31,32]

According to Figure 1, the stern part is composed of a pressure hull (end compartment) and a light hull. The slope of the stern shape has to be acceptable to arrange all items of equipment with a reasonable clearance in order to provide a satisfactory accessibility with respect to inspection, maintenance and repair. Most part of the stern is occupied by the main ballast tank (MBT) which requires a huge volume inside the stern. The more length of stern is equal to the best hydrodynamic conditions and the worse condition for the length of the propulsion shaft. There are several recommendations for the stern length such as IHSS,[6] but another important subject is correlated to the curvature and the submarine stern shape, especially in the light hull section. The main focus of this study is on the curvature and the shape equation of the stern. Submarines consist of two major categories of hydrodynamic shape: a teardrop shape and a cylindrical middle-body shape.

Because most of the real naval submarines contain cylindrical middle-body shape, the main part of this study is concentrated on the optimum hydrodynamic shape of the stern of cylindrical middle-body submarine. It is based on the minimum resistance with respect to the curvature and the equation of submarine stern shape, for example, in IHSS series.[6]

Submarines consist of two modes of navigation: surface mode and submerged mode. In the surface mode of navigation, the energy source limitation is lower than the submerged mode. Therefore, in terms of the real naval submarines, the determination of the required power of propulsion engines is based on the submerged mode. The focus of the recent research has been on the resistance at fully submerged mode with no regard of free surface effects.

Equations of stern form

a) Parabolic: this stern shape is not the blunt shape. The parabolic series shape is generated by rotating a segment of a parabola around an axis. This construction is similar to that of the tangent ogive, except that a parabola is the defined shape rather than a circle. This construction, according to Figure 2(a), produces a stern shape with a sharp tip, just as it does on an ogive case. For $0 \leqslant K' \leqslant 1$

$$y = R\left(\frac{2\left(\frac{x}{L}\right) - K'\left(\frac{x}{L}\right)^2}{2 - K'}\right) \quad (1)$$
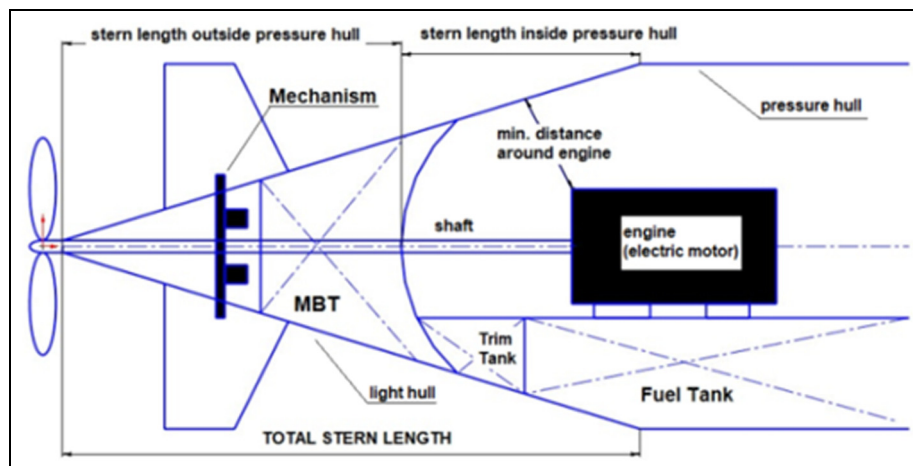

Figure 1. General arrangement of stern part (inside and outside of the pressure hull).
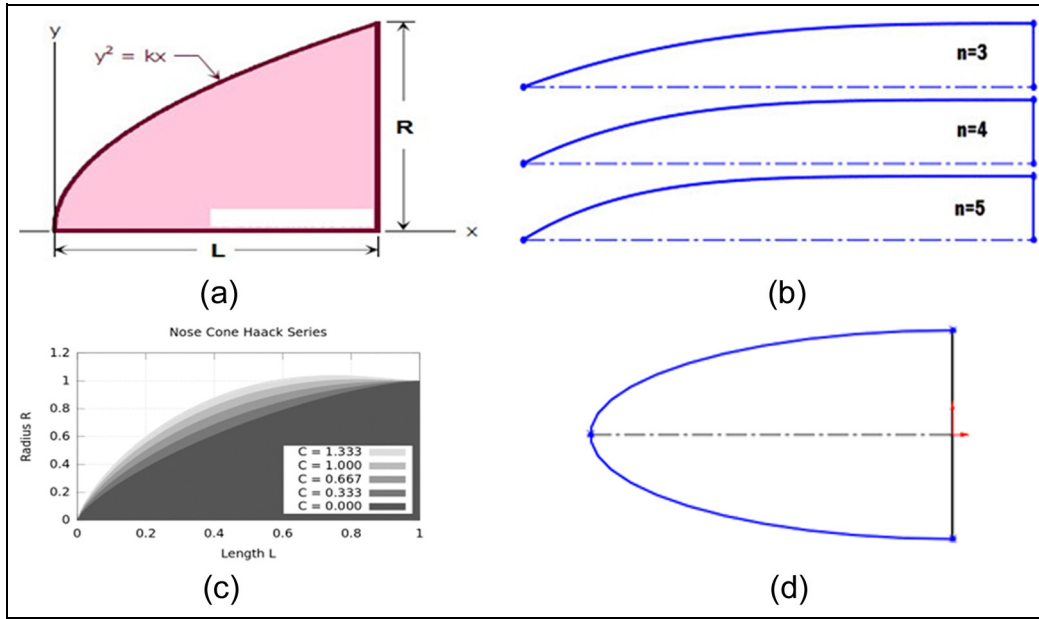
Figure 2. Several shapes of stern:[33,34] (a) parabolic stern, (b) power series for stern, (c) Haack series for stern shape and (d) elliptical stern.

K' can be set anywhere between 0 and 1, but the values most commonly used for stern shapes are as follows: $K' = 0$ for a cone, $K' = 0.5$ for a 1/2 parabola, $K' = 0.75$ for a 3/4 parabola and $K' = 1$ for a full parabola. For the case of full parabola ($K' = 1$), the shape is tangent to the body at its base and the base is on the axis of the parabola. Those values of "K'" that are less than 1 result in a slimmer shape, whose appearance is similar to that of the secant ogive. The shape is no longer tangent at the base, and the base is parallel to, but offset from, the axis of the parabola.

b) Power series: according to Figure 2(b), the power series includes the shape commonly referred to as a "parabolic" stern, but the shape correctly known as a parabolic stern is a member of the parabolic series (described above). The power series shape is characterized by its tip (usually blunt tip) and the fact that its base is not tangent to the body tube. There is always a discontinuity at the joint between stern and body that looks distinctly non-hydrodynamic.

The shape is able to be modified basically to smooth out this discontinuity. Not only a flat-faced cylinder but also a cone is included as some shapes that are members of the power series. The after body is generated by revolving a line around an axis that is described by equation (2)

$$Y_a = R \left[1 - \left(\frac{X_a}{L_a} \right)^{n_a} \right] \qquad (2)$$

The factor "n_a" controls the bluntness of the shape. Then for n_a, it can be said that $n_a = 1$ for a cone, $n_a = 2$ for a elliptic and $n_a = 0$ for a cylinder.

c) Haack series: despite all the stern shapes above, the Haack series shapes are not constructed from geometric figures. The shapes are mathematically derived from minimizing resistance instead. While the series is a continuous set of shapes determined by the value of C in the equations below, two values of C possess a particular significance: when $C = 0$, the notation LD signifies minimum drag for the given length and diameter, and when $C = 1/3$, LV indicates minimum resistance for a given length and volume. The Haack series shapes are not perfectly tangent to the body at their base, except for a case where $C = 2/3$. However, the discontinuity is usually too slight to be imperceptible. For $C > 2/3$, Haack stern bulge to a maximum diameter is greater than the base diameter. Haack nose tips do not lead to a sharp point, but are slightly rounded (Figure 2(c))

$$\theta = arccos \left(1 - \frac{2x}{L} \right) y = \frac{R}{\sqrt{\pi}} \sqrt{\theta - \frac{\sin(2\theta)}{2} + C\sin^3\theta}$$

$$(3)$$

where $C = 1/3$ for LV-Haack and $C = 0$ for LD-Haack.

d) Von Karman: the minimum drag, under the assumption of constant length and diameter, is offered by the Haack series. LD-Haack is commonly referred to as the Von Karman or the Von Karman ogive.

e) Elliptical: according to Figure 2(d), this shape of the stern is an ellipse, with the major axis being the centerline and the minor axis being the base of the stern. A body that is generated by a rotation of a full ellipse about its major axis is called a prolate spheroid, so an elliptical stern shape would properly be known as a

Table 1. Main assumptions of the models.

v (m/s)	L_t (m)	L_f (m)	L_m (m)	L_a (m)	D (m)	L_t/D	A_0 (m^2)
10	8	2	1	5	1	8	3.14
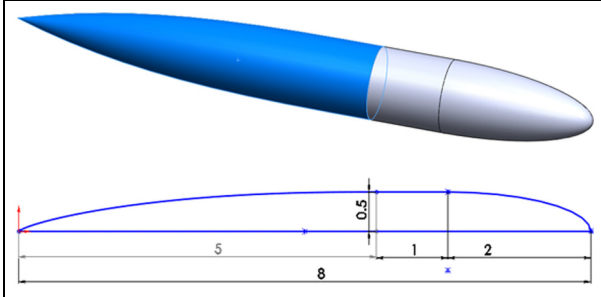
Figure 3. General configuration of the models, dimensions unit (m).

Figure 4. Configurations of parabolic models.

prolate hemispheric. This is not a shape normally found in the usual submarines. If R is equal to L, then the shape will be a hemisphere

$$y = R\sqrt{1 - \frac{x^2}{L^2}} \qquad (4)$$

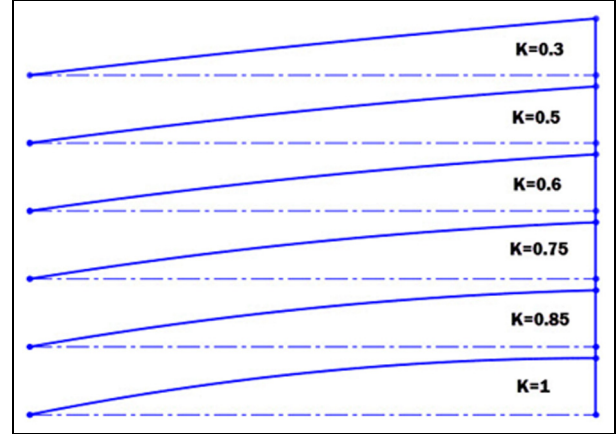## General assumptions for the models

Because the effect of the stern on resistance is only intended to be studied in this study, the base model considered in this task is an axisymmetric body (similar to torpedo) with no appendages. It helps model quarter of the body (in CFD model) and saves the time. The bow is elliptical and the middle part is cylindrical, but the stern part is different.

In this article, 19 models are studied. The three-dimensional (3D) models and their properties are modeled in SolidWorks (Figure 3). There are three main assumptions:

Assumption 1: to evaluate the hydrodynamic effects of the stern, the length of the stern is unusually supposed larger than usual. It helps effects of the stern to be more visible.
Assumption 2: for all the models, the shapes of bow and middle part are assumed to be constant. The bow is elliptical and the middle part is cylindrical.
Assumption 3: to provide a more equal hydrodynamic condition, the total length and the lengths of a bow, middle part and stern are assumed to be constant. The fineness ratio (L/D) is constant as well according to the constant status of the maximum diameter. The assumed constant parameters provide an equal form of resistance except for the stern shape that varies in each model. Consequently, the effects of the stern shape can

be analyzed and the models contained various volumes and wetted surface areas.

The main assumptions of all considered models are reported in Table 1. The specifications of all 19 models are presented in Figure 3 and reported in Table 2.

The wetted surface area (A_w) is used for the resistance coefficient and the total volume is used for "Semnan" coefficient. For all models, the volume of the bow and cylinder is constant which is equal to 1.83 m^3, but the total volumes are not the same. In addition, for CFD modeling in relation to all models, the velocity is assumed to be constant and equal to 10 m/s. In this study, the velocity is selected in which the Reynolds number could be more than 5 million. Based on this, according to Jackson and Capt,[19] where the Reynolds number is more than 5 million the total resistance coefficient remains unchanged.

The configurations of all models including parabolic models (Models 1-1 to 1-6), power series models (Models 2-1 to 2-9) and Haack series models (Models 3-1 to 3-4) are displayed in Figures 4–6, respectively.

CFD method of study

Governing equations

Transfer of momentum between layers is due to the following:

1. Viscosity or friction between fluid layers results in transfer of momentum from one fluid layer to another; this is a molecular level effect (due to rubbing of adjacent molecules).
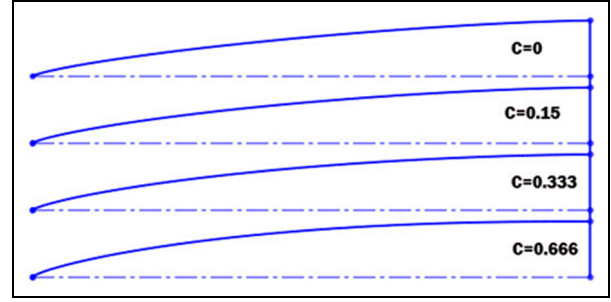
Table 2. Specifications of 19 models.

Model	Specification of stern	V (m³)
Model 1-1	Parabolic with $k' = 0.3$	3.26
Model 1-2	Parabolic with $k' = 0.5$	3.37
Model 1-3	Parabolic with $k' = 0.6$	3.45
Model 1-4	Parabolic with $k' = 0.75$	3.58
Model 1-5	Parabolic with $k' = 0.85$	3.7
Model 1-6	Parabolic with $k' = 1$	3.93
Model 2-1	Power series, $n = 1.5$	3.6
Model 2-2	Power series, $n = 1.65$	3.71
Model 2-3	Power series, $n = 1.85$	3.84
Model 2-4	Power series, $n = 2$ (elliptic)	3.93
Model 2-5	Power series, $n = 3$	4.36
Model 2-6	Power series, $n = 4$	4.63
Model 2-7	Power series, $n = 5$	4.81
Model 2-8	Power series, $n = 6$	4.94
Model 2-9	Power series, $n = 8$	5.12
Model 3-1	Haack series with $c = 0$	3.8
Model 3-2	Haack series with $c = 0.15$	3.91
Model 3-3	Haack series with $c = 0.333$	4.04
Model 3-4	Haack series with $c = 0.666$	4.29
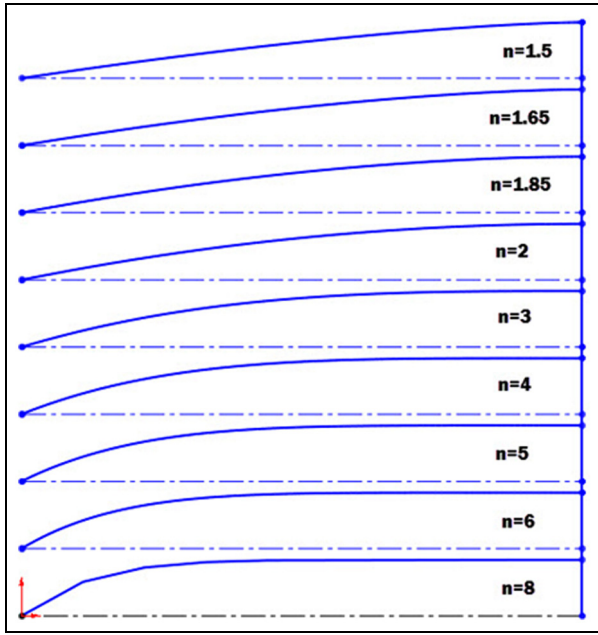
Figure 5. Configurations of power series models.

Figure 6. Configurations of Haack series models.

2. Turbulent mixing resulting in additional apparent stress or Reynolds stresses (after Osburn Reynolds in 1880s); this is a macroscopic effect due to bulk motion of fluid elements.

Momentum (Navier–Stokes) equation (three components in Cartesian coordinates) in conservative form is as equation (5)

$$\rho\left[\frac{\partial u}{\partial t} + \frac{\partial(u^2)}{\partial x} + \frac{\partial(uv)}{\partial y} + \frac{\partial(uw)}{\partial z}\right]$$
$$= -\frac{\partial p}{\partial x} + \frac{\partial}{\partial x}\left(\mu\frac{\partial u}{\partial x}\right) + \frac{\partial}{\partial y}\left(\mu\frac{\partial u}{\partial y}\right) + \frac{\partial}{\partial z}\left(\mu\frac{\partial u}{\partial z}\right)$$

$$\rho\left[\frac{\partial v}{\partial t} + \frac{\partial(vu)}{\partial x} + \frac{\partial(v^2)}{\partial y} + \frac{\partial(vw)}{\partial z}\right]$$
$$= -\frac{\partial p}{\partial y} + \frac{\partial}{\partial x}\left(\mu\frac{\partial v}{\partial x}\right) + \frac{\partial}{\partial y}\left(\mu\frac{\partial v}{\partial y}\right) + \frac{\partial}{\partial z}\left(\mu\frac{\partial v}{\partial z}\right)$$

$$\rho\left[\frac{\partial w}{\partial t} + \frac{\partial(wu)}{\partial x} + \frac{\partial(wv)}{\partial y} + \frac{\partial(w^2)}{\partial z}\right]$$
$$= -\frac{\partial p}{\partial z} + \frac{\partial}{\partial x}\left(\mu\frac{\partial w}{\partial x}\right) + \frac{\partial}{\partial y}\left(\mu\frac{\partial w}{\partial y}\right) + \frac{\partial}{\partial z}\left(\mu\frac{\partial w}{\partial z}\right)$$

$$(5)$$

Another form by using Einstein notation (sum each repeated index over i, j and k) for Cartesian coordinates and the x-component where $(x_i, x_j, x_k) = (x, y, z)$ and $(u_i, u_j, u_k) = (u, v, w)$ is as equation (6)

$$\rho\left[\frac{\partial(u_i)}{\partial t} + \frac{\partial(u_j u_i)}{\partial x_j}\right] = -\frac{\partial p}{\partial x_i} + \frac{\partial}{\partial x_j}\left(\mu\frac{\partial u_i}{\partial x_j}\right) \qquad (6)$$

In terms of shear stress by using $\tau_{ij} = \mu((\partial u_i/\partial x_j) + (\partial u_j/\partial x_i))$, or mean strain rate, $S_{ij} = \tau_{ij}/(2\mu)$, the equation is reformed to equation (7)

$$\rho\left[\frac{\partial(u_i)}{\partial t} + \frac{\partial(u_j u_i)}{\partial x_j}\right] = -\frac{\partial p}{\partial x_i} + \frac{\partial\tau_{ji}}{\partial x_j} \text{ or}$$
$$\rho\left[\frac{\partial(u_i)}{\partial t} + \frac{\partial(u_j u_i)}{\partial x_j}\right] = -\frac{\partial p}{\partial x_i} + \frac{\partial}{\partial x_j}(2\mu S_{ji})$$

$$(7)$$

The mean and fluctuating velocities and pressure can be represented as $u_i(x, y, z, t) = \bar{u}_i(x, y, z) + u_i'(x, y, z, t)$ and $p(x, y, z, t) = \bar{p}(x, y, z) + p'(x, y, z, t)$. The mean velocity is defined as

$$\bar{u} = \frac{1}{T}\int_0^T u_t dt$$

Substitute in mean and fluctuating variables and expand to get the form of equation (8)

$$\rho\left\{\frac{\partial(\bar{u}_i + u_i')}{\partial t} + \frac{\partial\left[(\bar{u}_j + u_j')\cdot(\bar{u}_i + u_i')\right]}{\partial x_j}\right\}$$
$$= -\frac{\partial(\bar{p} + p')}{\partial x_i} + \frac{\partial}{\partial x_j}\left[\mu\frac{\partial(\bar{u}_i + u_i')}{\partial x_j}\right]$$

$$\rho\left[\frac{\partial\bar{u}_i}{\partial t} + \frac{\partial(u_i')}{\partial t} + \frac{\partial(\bar{u}_j\bar{u}_i)}{\partial x_j} + \frac{\partial(\bar{u}_j u_i')}{\partial x_j} + \frac{\partial(\bar{u}_i u_j')}{\partial x_j} + \frac{\partial(u_j'u_i')}{\partial x_j}\right]$$

$$= -\frac{\partial\bar{p}}{\partial x_i} - \frac{\partial p'}{\partial x_i} + \frac{\partial}{\partial x_j}\left[\mu\frac{\partial\bar{u}_i}{\partial x_j} + \frac{\partial u_i'}{\partial x_j}\right] \qquad (8)$$

The following rules would be applied on the equations

$$\overline{\bar{u}_i} = \bar{u}_i \quad \overline{\bar{u}_i + u_i'} = \bar{u}_i + \overline{u_i'} = \bar{u}_i \quad \overline{\bar{u}_i \cdot u_i'} = \bar{u}_i \cdot \overline{u_j'} = 0$$

$$\overline{\frac{\partial\bar{u}_i}{\partial x_j}} = \frac{\partial\bar{u}_i}{\partial x_j} \quad \overline{\bar{u}_i^2} = \bar{u}_i^2 \quad \overline{u_i'u_j'} < 0$$

$$\frac{\partial u}{\partial t} = \frac{\partial\bar{u}}{\partial t} + \frac{\partial u'}{\partial t} \quad \frac{\partial}{\partial x}(u^2) = \frac{\partial}{\partial x}\left[(\bar{u} + u')^2\right]$$

$$= \frac{\partial}{\partial x}(\bar{u}^2 + 2\bar{u}u' + u'^2)$$

Many terms cancel to give Reynolds averaged Navier–Stokes (RANS) equations asequation (9)

$$\rho\left[\frac{\partial\bar{u}_i}{\partial t} + \frac{\partial(\bar{u}_j\bar{u}_i)}{\partial x_j}\right] = -\frac{\partial\bar{p}}{\partial x_i} + \frac{\partial}{\partial x_j}\left[\mu\left(\frac{\partial\bar{u}_i}{\partial x_j}\right) - \rho\overline{u_j'u_i'}\right]$$

$$\rho\left[\frac{\partial\bar{u}_i}{\partial t} + \frac{\partial(\bar{u}_j\bar{u}_i)}{\partial x_j}\right] = -\frac{\partial\bar{p}}{\partial x_i} + \frac{\partial}{\partial x_j}(2\mu\bar{S}_{ji} - \rho\overline{u_j'u_i'}) \quad (9)$$

The term $(-\rho\overline{u_i'u_j'})$ is named Reynolds stresses. Reynolds stresses are positive because the velocity fluctuations are correlated through conservation of mass such that $\overline{u_i'u_j'} < 0$. Reynolds stresses include nine elements (only six independent) due to $\tau'_{ij} = \tau'_{ji} = -\rho\overline{u_i'u_j'}$ (where i = j for normal stress) as equation (10)

$$\overline{u_i'u_j'} = \begin{bmatrix} \overline{u'^2} & \overline{u'v'} & \overline{u'w'} \\ \overline{v'u'} & \overline{v'^2} & \overline{v'w'} \\ \overline{w'u'} & \overline{w'v'} & \overline{w'^2} \end{bmatrix} \qquad (10)$$

There are seven unknowns (six unknowns for velocities and one for pressure) but four equations (three Navier–Stokes and one continuity). Therefore, there are three transfer equations such as turbulent models such as k–ε. The eddy viscosity is also commonly called the turbulent viscosity and it is normally written as μ_t. Turbulent viscosity is defined based on Reynolds stress as $\tau_t = -\rho\overline{u'v'} = \mu_t(\partial u/\partial y)$.

Therefore, $\tau = \tau_o + \tau_t = (\mu_o + \mu_t)(\partial u/\partial y)$ and $\mu = \mu_o + \mu_t$ where μ_o is the viscosity of laminar flow and μ_t is the turbulent viscosity. For calculation of μ_t, two kinds of turbulent models are used: (1) eddy viscosity essential equations such as Boussinesq, Speziale and Launder. (2) Eddy viscosity models included six models: standards k–ε, extended k–ε, re-normalization group (RNG) k–ε, anisotropic k–ε, Wilcox k–ω and shear stress transport (SST) k–ω. In this study, the following equations are employed: Boussinesq and standards k–ε model. Boussinesq equation is stated as

$$-\rho\overline{u_i'u_j'} = 2\mu_t S_{ij} - \frac{2}{3}\rho k\delta_{ij}$$

And finally for the calculation of μ_t, the model standards k–ε uses two parameters of k and ε

$$k = \frac{1}{2}\overline{u_i'u_i'}, \varepsilon = \left(\frac{\mu}{\rho}\right)\overline{u_{i,j}'u_{i,j}'}, \mu_t = C_\mu\rho\frac{k^2}{\varepsilon}$$

All terms of these equations are represented in Sanieenezhad.[35]

Meshing, boundary conditions and domain description

This analysis is conducted by Flow Vision (V.2.3) software based on CFD method and solving the RANS equations. The validity of this software has been done by several experimental test cases and, nowadays, this software is accepted as a practical and reliable software in CFD activities. Finite volume method (FVM) is used for modeling the cases which are considered in this article. One structured mesh with cubic cell has been used for mapping the space around the submarine. To monitor and model the boundary layer near the solid surfaces, the selected cells near the object in comparison with the other parts of domain are tiny and very small. To single out the proper number of the cells, for one certain model (Model 2-4) and v = 10 m/s, five different amounts of meshes were selected and the results were compared insofar as the results remained almost constant after 1.5 million mesh points which shows the results are not dependent on the mesh size (Figure 7). In all models, the mesh numbers are considered more than 2 million.

For an appropriate convergence, the iteration process is kept on until the tolerance of convergence (less than 1%) will be considered to be satisfactory. All iterations are continued to be more than 1 million. The following characteristics are used in this domain: inlet with a uniform flow, free outlet, symmetry in the four faces of the box and wall for the body of submarine. The dimensions of cubic domain for this sample case are as follows: length = 56 m (equal to 7L), beam = 8 m (equal to L or 8D) and height = 8 m (equal to L or 8D). Due to axisymmetry, only a quarter of the body is considered in numerical computation. This leads to a
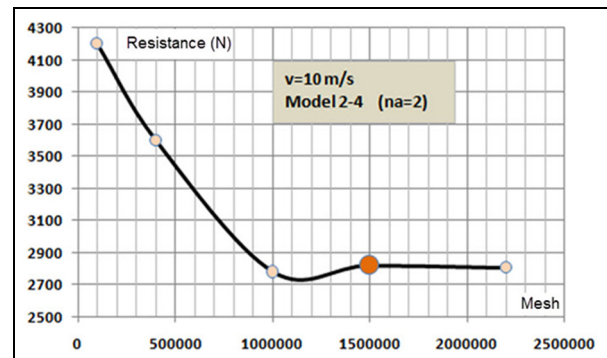

Figure 7. Mesh independency evaluations.

Table 3. Settings of the domain simulation.

Elements	Boundary conditions	Descriptions	
Domain	Box	Conditions	Fully submerged modeling (without free surface), quarter modeling, domain with inlet, outlet, symmetry and wall, without heat transfer.
		Dimensions	56 × 8 × 8 m, length before and after model = 16 and 32 m.
		Meshing	Structured grid, hexahedral cells, tiny cell near wall, meshes more than 2 million.
		Settings	Iterations more than 1500, time step = 0.01 s.
Fluid	–		Incompressible fluid, Reynolds number more than 24 million, turbulent modeling: standard k–ε, fresh water, temperature: 20 °C, ρ = 999.841 kg/m^3.
Object	Wall		Bare hull of submarine: value 30 $<$ y^+ $<$ 100, roughness = 0, no slip.
Input	Inlet		Velocity = 10 m/s, constant, normal (along x), in one face.
Output	Free outlet		Zero pressure, in one face.
Boundaries	Symmetry		In four faces.

significant saving in the computation time. Meanwhile, this study has shown that the length of the beam and height equal to 8D can be acceptable in this consideration. Here, there is no need for fine meshes far away from the object. The forward distance of the model is equal to 2L and after distance is 4L in the total length of 7L (Figure 8). The turbulence model is k–ε and y^+ is considered equal to 30.

The considered flow is incompressible fluid flow (fresh water) at 20 °C and a constant velocity of 10 m/s. Time step of each iteration depends on the model length and velocity, so here time step is defined equal to 0.01 s. The settings of the simulation are collected in Table 3.

CFD result analysis. CFD analyses were conducted for all 19 models by Flow Vision software under the above-mentioned conditions. All results are obtained at fully submerged mode with no regard of free surface effects. The total resistance takes the effects of pressure distribution and viscosity into account. Therefore, the total resistance is the summation of pressure (form) resistance and viscose (frictional) resistance. Pressure contours around the body are shown in Figure 9 for sample for Model 1-1. The fore part of this object includes stagnation point and high-pressure area. The middle part is the low-pressure area, but the stern part is the high-pressure area. The pressure distribution on the body is non-uniform. This leads to the pressure resistance. If the stern design can be conducted to a streamlined form, then the high-pressure area in the aft part is reduced and causes lower pressure resistance. This means that the optimally designed stern results in a lesser pressure in the stern part.

In viscose resistance, an important parameter is the wetted area resistance. This parameter varies in all models, but the cross-sectional area remains fixed, because the diameter is constant in all models. The values of wetted area are reported in Table 2. For better comparison, they are displayed in Figure 10 as well.

Based on the area, two kinds of the resistance coefficient can be defined: (1) based on the wetted area:
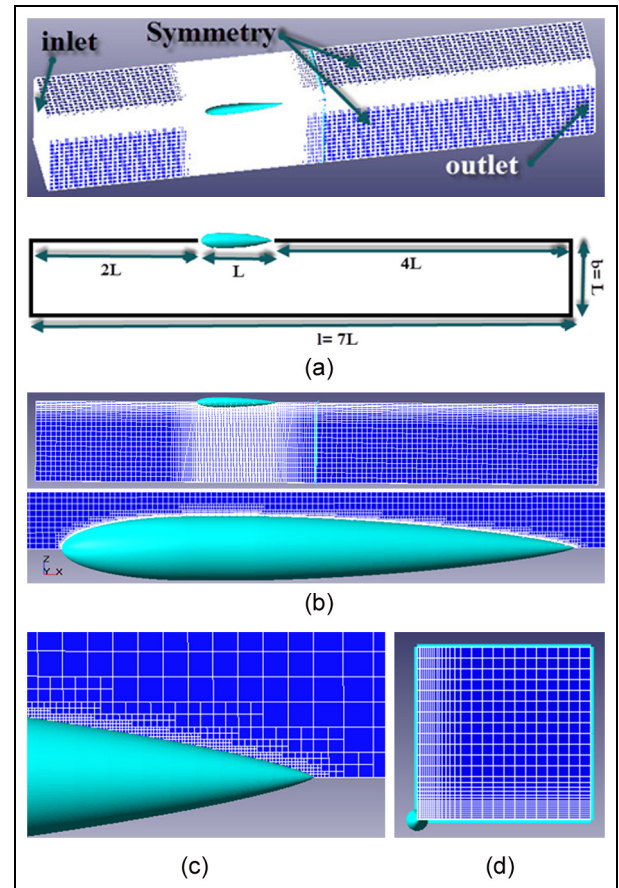

Figure 8. (a) Domain dimensions, (b) domain and structured grid, (c) very tiny cells near the wall for boundary layer modeling and keeping y + about 30 and (d) quarterly modeling because of axisymmetry.

$C_{d1} = R/(0.5\rho A_w v^2)$ that is usually used for the frictional resistance coefficient. (2) Based on the cross-sectional area: $C_{d0} = R/(0.5\rho A_0 v^2)$ that is usually used for the pressure resistance coefficient. Here, for accounting the effect of the wetted area on the coefficients, all coefficients are presented as a function of the wetted area. The amount of total resistance and
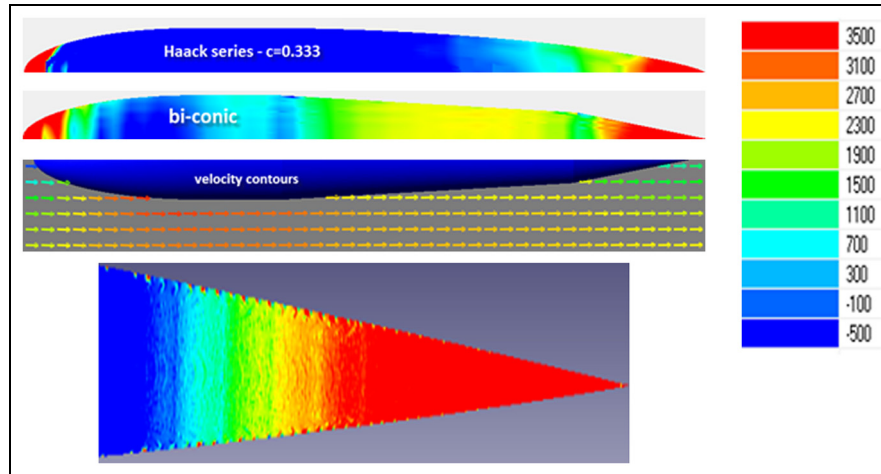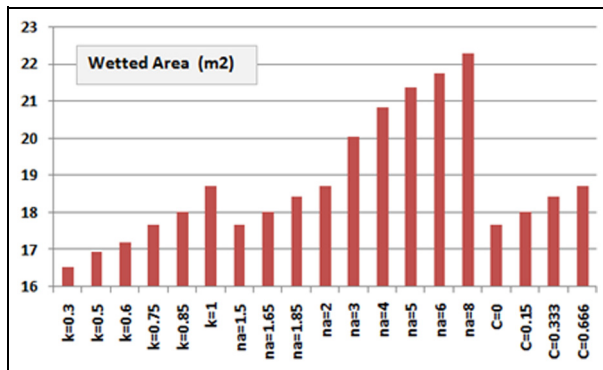
Figure 9. Pressure contour around the body.

Figure 10. Comparison of wetted area for 19 models.

Table 4. Total resistance, resistance coefficient (based on wetted area surface) and Semnan coefficient of the models.

Model	R_t (N)	$C_t \times 10,000$	$C_{semnan}/10$
Model 1-1	2472	29.87	37.71
Model 1-2	2510	29.60	39.01
Model 1-3	2528	29.38	39.97
Model 1-4	2577.2	29.19	41.28
Model 1-5	2614.8	29.02	42.44
Model 1-6	2692	28.78	44.49
Model 2-1	2688	30.44	39.73
Model 2-2	2716	30.16	40.91
Model 2-3	2760	29.95	42.13
Model 2-4	2808	30.02	42.65
Model 2-5	2940	29.36	46.40
Model 2-6	3024	29.04	48.53
Model 2-7	3120	29.21	49.24
Model 2-8	3220	29.61	49.28
Model 2-9	3460	31.07	47.85
Model 3-1	2780	31.48	40.27
Model 3-2	2824	31.36	41.16
Model 3-3	2868	31.12	42.31
Model 3-4	2960	31.64	43.18

resistance coefficient is presented in Table 4. In this study, an ideal stern form should have minimum resistance. It should be remembered that here there are two main parameters as follows: (1) the wetted area which affects the frictional resistance and (2) the general form which affects the pressure resistance by better distribution of pressure on the body and avoiding low-pressure area in the aft part of the body.

Resistance and volume are the two main parameters that affect the stern shape design. The coefficient that can describe both parameters is the Semnan coefficient that is defined as equation (11)

$$Semnan\ coefficient(Ksn) = \frac{(Volume)^{\frac{1}{3}}}{Resistance\ coefficient} \quad (11)$$

Semnan coefficient can be named "hydro-volume efficiency." For selecting a good shape form of submarine, this coefficient is a very important parameter because it counts both resistance and volume. The larger values of this coefficient provide better design. In some cases, under the assumption of constant length, a shape that has minimum resistance cannot be a good design with having a small volume (such as a simple conical stern). Regarding this coefficient, the stern

volume instead of the total volume of submarine is taken into account, because the focus here is on the stern design.

The diagrams of the total resistance, resistance coefficient and Semnan coefficients corresponding to the Parabolic, power series and Haack series sterns are shown in Figures 11–13, respectively. In the parabolic stern form, according to Figure 11, the total resistance increases and the resistance coefficient decreases with an increase in K′. It means that under the assumption of constant length, the lesser value of K′ is better, and under the assumption of constant wetted surface area, a higher value of K′ is better. For having a better criteria, from view point of naval architecture design, Semnan coefficient needs to be higher for providing simultaneously lesser value of resistance coefficient and a higher value of enveloped volume. Here, a higher
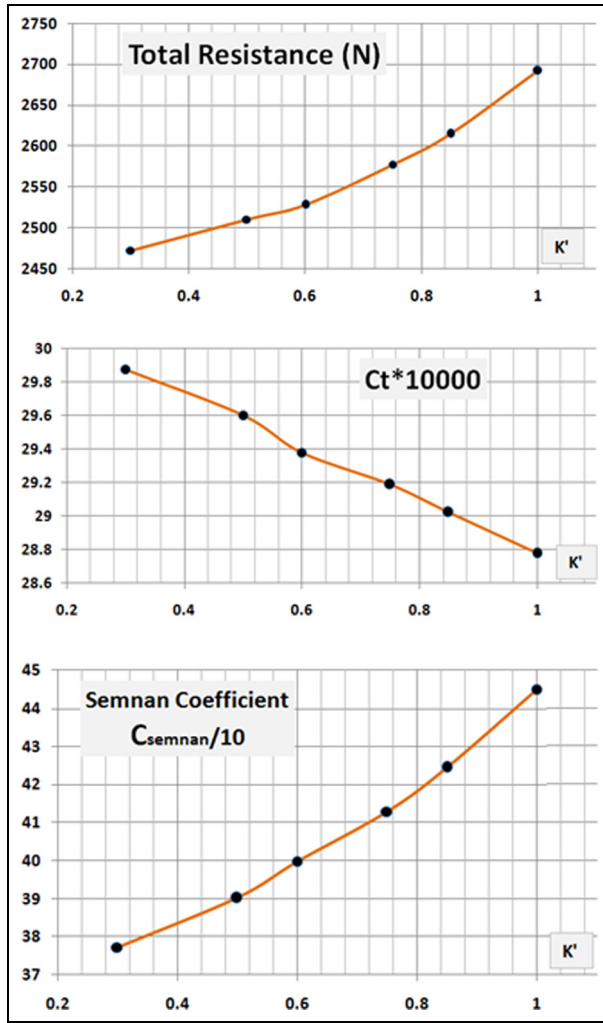
Figure 11. Variation in the total resistance, resistance coefficient and Semnan coefficient with K′ for parabolic stern.

Figure 12. Variation in the total resistance, resistance coefficient and Semnan coefficient with n_a for power series stern.

value of K′ means a higher value of Semnan coefficient and a better condition as well. The equation of resistance coefficient is stated as equation (12)

$$C_t = -1.572(K') + 30.35 \qquad (12)$$

In the power series stern form, according to Figure 12, the total resistance increases with an increase in n_a. The resistance coefficient diagram has two minimum points: a local minimum at $n_a = 1.85$ and a global minimum at $n_a = 4$. It means that under the assumption of constant length, the lesser value of n_a is better, but under the assumption of constant wetted surface area with regard to the resistance coefficient, the values of n_a around 4 are better. For this form, the Semnan coefficient has a maximum value around $n_a = 5.6$ that shows the best selection regarding design process.

In this regard, the equation of resistance coefficient for $2 < n_a < 8$ is as equation (13)

$$C_t = -0.01(n_a)^3 + 0.33(n_a)^2 - 2.11(n_a) + 33.03 \qquad (13)$$

In the Haack series stern form, according to Figure 13, the total resistance increases with an increase
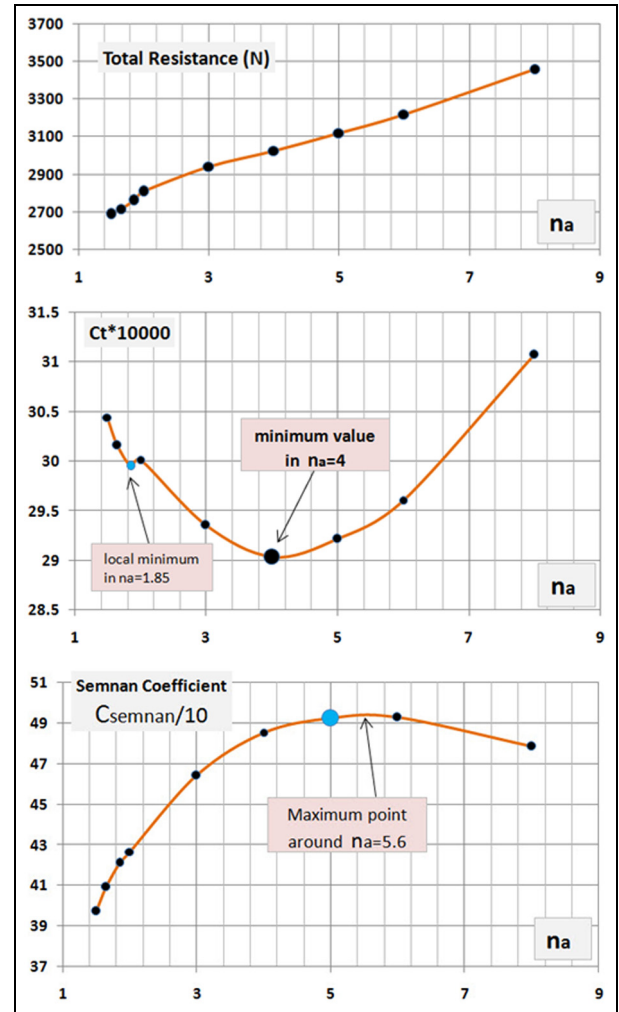
in C. This variation is exactly linear. It means that under the assumption of constant length, the lesser value of C is better, but under the assumption of constant wetted surface area with regard to the resistance coefficient, the values of C around 0.3 are better. For this form, the Semnan coefficient increases with an increase in "C." In this regard, the equation of resistance coefficient is as follows

$$C_t = 30.9839 + 0.2066 \cos(9.176C + 0.1161) \qquad (14)$$

Conclusion

In conclusion, the results of this study can be stated as follows:

1. In the parabolic stern form, under the assumption of constant length, the value of K′ = 0.3 is a good selection, but under the assumption of constant wetted surface area, the stern form with K′ = 1 is
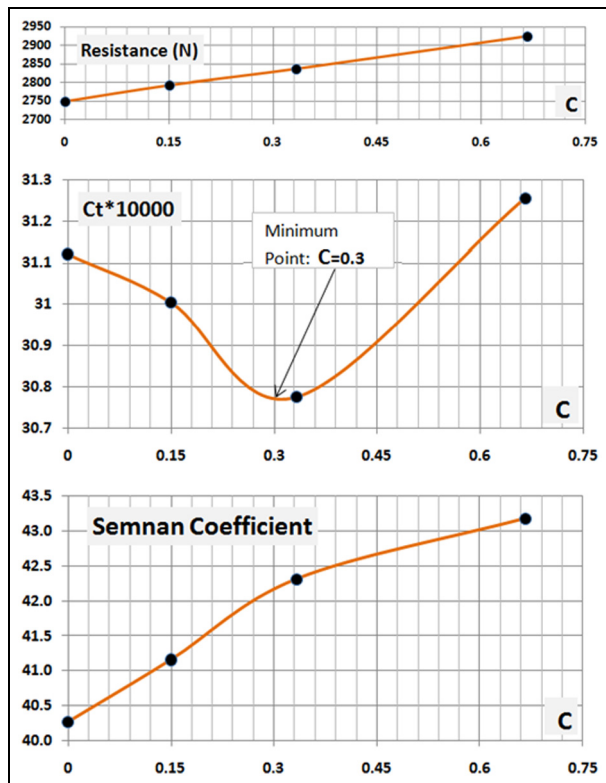
Figure 13. Variation in the total resistance, resistance coefficient and Semnan coefficient with C for Haack series stern.

the best design, because the maximum value of Semnan coefficient is achieved in this value.

2. In the power series stern form, under the assumption of constant wetted surface area, there are two minimum points around $n_a = 1.85$ and 4 which offer good selections, but under the assumption of constant length, the stern form with $n_a = 5.6$ is the best design, because the maximum value of Semnan coefficient is achieved in this value.

3. In the Haack series stern form, under the assumption of constant wetted surface area, the value of $C = 0.3$ is a good selection because the minimum resistance coefficient is achieved in this value. Under the assumption of constant length, the stern form with $C = 0.66$ is the best design because higher values of C are equal to higher values of Semnan coefficient.

4. A comparison between the three types of stern shapes, under the assumption of constant wetted surface area, indicates that the Haack series stern form has the worse result by the most value of resistance coefficient. The power series stern form, under the assumption of constant length, has the worse result by the most value of resistance. For providing more volume with the lesser resistance coefficient, based on the maximum value of Semnan coefficient, the power series stern form has the most value and offers the best result.

5. Finally, the best advice of this article for the stern form of submarine based on the diagrams of

Semnan coefficients is "power series" in the range of 4–6 for n_a.

References

1. Joubert PN. *Some aspects of submarine design: part 1—hydrodynamics*. Australian Department of Defence, 2004, http://www.dtic.mil/cgi-bin/GetTRDoc?AD = ADA428039
2. Joubert PN. *Some aspects of submarine design: part 2—shape of a submarine 2026*. Australian Department of Defence, 2004, http://dtic.mil/cgi-bin/GetTRDoc?AD = ADA470163
3. Burcher R and Rydill LJ. *Concept in submarine design*. Cambridge: The Press Syndicate of the University of Cambridge, Cambridge University Press, 1998, p.295.
4. Yuri NK and Oleg AK. *Theory of submarine design*. Saint Petersburg: Saint Petersburg State Maritime Technical University, 2001, pp.185–221.
5. Moonesun M, Javadi M, Charmdooz P, et al. Evaluation of submarine model test in towing tank and comparison with CFD and experimental formulas for fully submerged resistance. *Indian J Geoma Sci* 2013; 42(8): 1049–1056.
6. Moonesun M. Introduction of Iranian Hydrodynamic Series of Submarines (IHSS). *J Taiwan Soc Naval Archit Mar Eng* 2014; 33(3): 155–162.
7. Moonesun M and Korol YM. Concepts in submarine shape design. In: *Proceedings of the 16th marine industries conference (MIC2014)*, Bandar Abbas, Iran, 2–5 December, 2014. Iranian Association of Naval Architecture and Marine Engineering (IRANAME).
8. Moonesun M, Korol YM and Brazhko A. CFD analysis on the equations of submarine stern shape. *J Taiwan Soc Naval Archit Mar Eng* 2015; 34(1): 21–32.
9. Moonesun M, Korol YM and Tahvildarzade D. Optimum L/D for submarine shape. *Indian J Geoma Sci*, in press.
10. Moonesun M, Korol YM, Tahvildarzade D, et al. Practical solution for underwater hydrodynamic model test of submarine. *J Korean Soc Mar Eng* 2014; 38(10): 1217–1224.
11. Iranian Defense Standard (IDS-857:2011). Hydrodynamics of medium size submarines.
12. Praveen PC and Krishnankutty P. Study on the effect of body length on hydrodynamic performance of an axisymmetric underwater vehicle. *Indian J Geoma Sci* 2013; 42(8): 1013–1022.
13. Suman KS, Nageswara RD, Das HN, et al. Hydrodynamic performance evaluation of an ellipsoidal nose for high speed underwater vehicle. *Jordan J Mech Ind Eng* 2010; 4(5): 641–652.
14. Mackay M. *The standard submarine model: a survey of static hydrodynamic experiments and semiempirical predictions*. Ottawa, ON, Canada: Defence R&D Canada, 2003, p.30.

15. Baker C. *Estimating drag forces on submarine hulls.* Ottawa, ON, Canada: Defence R&D Canada, 2004, p.131.
16. Alemayehu D, Boyle RB, Eaton E, et al. Guided missile submarine SSG(X): SSG(X) variant 2-44, ocean engineering design project, AOE 4065/4066, Virginia Tech team 3, 2005, pp.11–12, https://www.aoe.vt.edu/people/web-pages/albrown5/design/2006team3t30.pdf
17. Minnick L. *A parametric model for predicting submarine dynamic stability in early stage design.* Blacksburg, VA: Virginia Polytechnic Institute and State University, 2006, pp.52–53.
18. Grant BT. *A design tool for the evaluation of atmosphere independent propulsion in submarines.* Cambridge, MA: Massachusetts Institute of Technology, 1994, pp.191–193.
19. Jackson HA and Capt PE. Submarine parametrics. In: *Proceedings of the royal institute of naval architects international symposium on naval submarines*, London, 1983. London: Royal Institute of Naval Architects.
20. Stenars JK. *Comparative naval architecture of modern foreign submarines.* Cambridge, MA: Massachusetts Institute of Technology, 1988, p.91.
21. Prestero T. *Verification of a six-degree of freedom simulation model for the REMUS autonomous underwater vehicle.* Davis, CA: University of California, Davis, 1994, pp.14–15.
22. Myring DF. A theoretical study of body drag in subcritical axisymmetric flow. *Aeronaut Quart* 1976; 27: 186–194.
23. Hoerner SF. *Fluid dynamic drag.* Midland Park, NJ: Hoerner Fluid Dynamics, 1965.
24. Greiner L. *Underwater missile propulsion: a selection of authoritative technical and descriptive papers.* Arlington, VA: Compass Publications, 1968.
25. Denpol EV. *An estimation of the normal force and the pitching moment of "Teardrop" underwater vehicle*, 1976.
26. Groves NC, Haung TT and Chang MS. *Geometric characteristics of DARPA SUBOFF model.* Bethesda, MD: David Taylor Research Centre, 1989.
27. Roddy R. *Investigation of the stability and control characteristics of several configurations of the DARPA SUBOFF model (DTRC Model 5470) from captive-model experiment.* Defense Technical Information Center, Report no. DTRC/SHD-1298-08, September 1990.
28. Jerome SP, Raymond EG and Fabio RG. Shaping of axisymmetric bodies for minimum drag in incompressible flow. *J Hydronaut* 1974; 8(3): 100–108.
29. Brenden M. *Design and development of UUV.* Thesis Report, School of Engineering and Information Technology, University of New South Wales, Australian Defence Force Academy, Canberra, BC, Australia, 2010.
30. Volker B and Alvarez A. *Hull shape design of a snorkeling vehicle.* Esporles: Institut Mediterrani d'Estudis Avançats (IMEDEA), 2007.
31. Moonesun M, Korol YM and Dalayeli H. CFD analysis on the bare hull form of submarines for minimizing the resistance. *Int J Marit Technol* 2014; 3: 1–13.
32. Moonesun M, Korol YM, Tahvildarzade D, et al. CFD analysis on the equations of submarine bow shape. *J Korean Soc Mar Eng*, in press.
33. https://en.wikipedia.org/wiki/Nose_cone_design
34. Bronshtein IN, Semendyayev KA, Musiol G, et al. *Handbook of mathematics.* Berlin-Heidelberg: Springer, 2007.
35. Sanieenezhad M. *An introduction to turbulent flow and turbulence modeling.* Tehran, Iran: CFD Group Publication, 2003.

Appendix I

Notation

A_w	wetted area (outer area subject to the water) (m^2)
A_0	cross-sectional area ($3.14 \times D^2/4$) (m^2)
C_t	total resistance coefficient is shown in $\times 1000$
D	diameter of the cylinder part (or) radius of the base of the stern
Ksn	Semnan coefficient
L_a	stern length of submarine (m)
L_f	fore (bow) length of submarine (m)
L_m	middle part length of submarine (m)
L_t	total length of submarine (m)
R_t	total resistance (N)
v	speed of submarine (m/s)
V	total volume of submarine (m^3)
x	variable along the length, x varies from 0 to L
y	radius at any point x

Other parameters are described inside the text or in related references.